A novel analytical approach for the estimationof shear in the oscillatory membrane microfiltration

Article · March 2021

DOI: 10.1016/j.envc.2021.100066

4 authors, including:

Asmat Ullah
University of Engineering and Technology, Peshawar
35 PUBLICATIONS **209** CITATIONS
SEE PROFILE

Saad Ullah Khan
Ghulam Ishaq Khan Institute of Engineering Sciences and Technology
7 PUBLICATIONS **20** CITATIONS
SEE PROFILE

Kamran Alam
Ghulam Ishaq Khan Institute of Engineering Sciences and Technology
17 PUBLICATIONS **22** CITATIONS
SEE PROFILE

Environmental Challenges 4 (2021) 100066

Contents lists available at ScienceDirect

Environmental Challenges

journal homepage: www.elsevier.com/locate/envc

A novel analytical approach for the estimation of shear in the oscillatory membrane microfiltration

Asmat Ullah[a,*], Saad Ullah Khan[b], Kamran Alam[b], Hayat Khan[a]

[a] Department of Chemical Engineering, University of Engineering & Technology Peshawar, KPK Pakistan
[b] Faculty of Materials and Chemical Engineering, GIK Institute of Engineering Sciences and Technology, Topi, Pakistan

ARTICLE INFO

Keywords:
Shear rate
Membrane oscillation
Slotted pore membrane
Membrane fouling
Oil/water separation

ABSTRACT

A novel analytical approach for estimating the shear rate over the membrane surface and away from the membrane surface as a result of the membrane oscillation has been presented. The model was developed and modified according to our system using the Stokes boundary layer equation. Generation of the shear over the membrane surface is an important phenomenon that not only mitigates the fouling but also enhances the separation efficiency. It is investigated that membrane oscillating frequency, amplitude and viscosity of the souring fluid are important parameters that influence the intensity of the shear on the membrane surface and away from the surface. The model presented was tested with various set of frequencies, amplitudes and viscosities. While, keeping the amplitude constant and changing the frequencies, ahigherintensity of shear over the membrane surface was noticed. On the other hand, keeping the frequency constant and changing the amplitude, a lower shear on the membrane surface was observed. Similarly, as expected, a lower shear over the membrane surface was noticed when the viscosity of the surrounding fluid was increased. The model was supported with the experimental results where separation of oil drops from produced water was the focus of the experiments conducted. It was clear from the experimental results that membrane oscillation enhanced the separation efficiency of the membrane used and therefore, concentration of oil drops in the permeate decreased. Further, the application of the shear was greatly influenced by the pore blocking; higher the shear rate; lower was the pore blocking and vice versa.

1. Introduction

Oily wastewater is a major environmental concern that adversely impacts the sea water quality (Cheryan and Rajagopalan, 1998; Fakhru'l-Razi et al., 2009; Faksness et al., 2004; Jiménez et al., 2018). Oil and gas industry generate a large volume of oily wastewater and the annual estimation worldwide is about 88 billion barrels (Rezakazemi et al., 2018). Several separation techniques exist for handling oily wastewater, such as gravitational processes, pH adjustment, centrifuge, electrostatic de-emulsification (Dezhi et al., 1999; Eow et al., 2001), bio-treatment (Partovinia & Naeimpoor, 2013, 2014) and membrane filtration (Cheryan and Rajagopalan, 1998; Jepsen et al., 2018; Widodo et al., 2018; Y. Zhu et al., 2014). Membrane separation technologies are gaining popularity for the following reasons (Jepsen et al., 2018; Padaki et al., 2015):(i) no hazardous chemicals are needed in the process (ii) the process is environmentally friendly and (iii) produce highly quality of permeate.

Membrane technologyis more suitable for treating oily wastewater then other techniques(Bilstad and Espedal, 1996; Patterson, 1985). Despite usefulness of such applications, the major drawback for membrane separation of oil-water emulsions is fouling which leads to reduction in the volumes that can be treated (Huang et al., 2018; Jepsen et al., 2018).

In membrane processes, different techniques have been investigated to effectively separate oil drops from produced water, which is a byproduct during extraction of oil and gas. Microfiltration (MF) (Cumming et al., 2000; Holdich et al., 1998; Nazzal and Wiesner, 1996; Pope et al., 1996; Ullah et al., 2011, 2015; Ullah, Holdich, et al., 2012b) and ultra-filtration (UF) (Chakrabarty et al., 2008; Falahati and Tremblay, 2011; Lee et al., 1984; Lipp et al., 1988; Lu et al., 2015; Nabi et al., 2000)processes have been preferred for oil water separation over other membrane separation processes. Microfiltration and ultrafiltration havefilter pore size of 0.1 microns and 0.01 microns, respectively. The membrane fouling in microfiltration and ultra-filtration is lower as compared to the nano-filtration and reverse osmosis processes for treating oily streams. MFgives high permeate flux and low trans-membrane pressure and therefore could be economically beneficial on large scale as compared to UF(Mohammadi et al., 2003; Peng et al., 2004; Ullah, Khan, et al., 2013). Similarly, the effect of membrane pore geometry has been studied by many researchers (Chandler and Zydney, 2006; S Kuiper et al., 2002; Stein Kuiper et al., 2002; van Rijn et al., 1998). In recent

* Corresponding author.
E-mail address: a.ullah@uetpeshawar.edu.pk (A. Ullah).

https://doi.org/10.1016/j.envc.2021.100066
Received 5 January 2021; Received in revised form 21 February 2021; Accepted 23 February 2021

Nomenclature

A	Amplitude of Vibration (m)
F	Frequency (Hz (s^{-1}))
V	$A\omega$ (ms^{-1})
X(z,t)	Instantaneous displacement of an immersed body oscillating along z-axis (m)
T	Time (s)
V_y	Velocity of the fluid in y direction (ms^{-1})
V_z	Velocity of the fluid in z direction (ms^{-1})
Y	Lateral coordinates (m)
Z	Directional Coordinate (m)
γ	Shear rate (s^{-1})
$“\gamma_{(0)}$	Shear rate at membrane surface (s^{-1})
μ	Fluid Viscosity ($kgm^{-1}s^{-1}$)
υ	Fluid kinematic Viscosity (m^2s^{-1})
ρ	Fluid density (kgm^{-3})
ω	Angular Frequency ($rads^{-1}$)
i	Iota = $\sqrt{-1}$
$\Re e$	Real part of the equation

years, slotted pore membranes have been evaluated for the separation of oil content from produced water and were found effective in comparison to the circular pore membranes (Ullah et al., 2011, 2014, 2019; Ullah, Khan, et al., 2013; Ullah, Starov, et al., 2013).

Recently, shear enhanced MF for oil water emulsion has come to the attention of researchers globally. Different shear enhancement techniques, i.e., aeration and high cross-flow system, can reduce membrane fouling." Alleviate is better than reduce. In aeration system, bubbles are produced, that generate vortices and commotion to disperse the layer of concentration polarization and reduce fouling (Cui et al., 2003). But the major drawback of this technique is high power consumption. In cross-flow filtration, the fluid needs to be pump again and again into the process for the shear generation and utilize an extensive energy (Postlethwaite et al., 2004; Sarrade et al., 2001). To overcome the high-power consumption for the cross-flow filtration to create shear rate on membrane surface, another approach was studied called dynamic microfiltration, in which high shear rate is produced by relative movement between filtration module and bulk fluid. This relative motion is either achieved by vibrating or rotating the membrane module. It has been studied that concentration polarization and membrane fouling has been mitigated using membrane oscillation (Beier and Jonsson, 2007; Bellhouse et al., 1994; Genkin et al., 2006; Gomaa et al., 2004; Gomaa and Al Taweel, 2004, 2005; Gomaa & Taweel, 2007; Herman and Kang, 2001a, 2001b; Mackley and Stonestreet, 1995; Ni et al., 2003). Besides this, it also reduces the transmembrane pressure four times and also gives high rejection of oil drops. Moreover, membrane oscillation also results lower concentrations of oil in permeate. Oscillation of the membrane was therefore found to be useful at the small scale (Ullah et al., 2020).

The objective of the study was to evaluate the effect of membrane oscillation on the shear rate generation on the surface and away from the surface. For that purpose, a new analytical model has been developed that simultaneously counts the effect of oscillation frequency and amplitude on shear rate over membrane surface and in the fluid away from membrane surface. The model was developed based on the Stokes boundary layer equation. The model has been simulated computationally to investigate shear rate at the membrane surface with different sets of oscillation amplitudes and frequencies. The shear rate was found to be a function of oscillating frequencies, amplitudes as well as fluid kinematic viscosity. The developed model for membrane oscillation has been simulated through MATLAB and validated with experimental data.

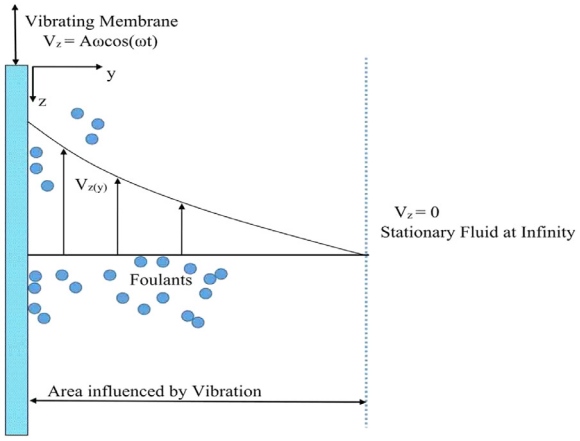

Fig. 1. Fluid distribution and foulants movement in submerged vibrating membrane.

2. Model formulation

Fig. 1 represents the submerge membrane vibrating along vertical z –axis. A velocity gradient was produced due to the oscillation/vibration of membrane along y direction that is referred asthe shear rate. Membrane vibration helps to push away fouling material from the membrane surface and commotion has produced in the bulk fluid and a consequence reduces fouling and concentration polarization. A mathematical model has been developed to represent the shear rate generating at membrane surface due to oscillation of membrane. The membrane is assumed as a plate surface to make the system for Cartesian co-ordinate analysis. As presented in Eq. (1), the Navier stoke equation was modified according to the system as (Salon et al., 2007):

$$\frac{\partial V_z}{\partial t} = \frac{\mu}{\rho}\left(\frac{\partial^2 V_z}{\partial y^2}\right) \tag{1}$$

To develop boundary conditions, the instantaneous displacement of an immersed body oscillating along z-axis from its rest position is given by;

$$X_{(z,t)} = A\sin(\omega t)$$

Then

B.C.1 : at $y = 0$ $\quad V_z = A\omega\cos(\omega t)$
B.C.2 : at $y \to \infty$ $\quad V_z = 0$

2.1. Derivation of shear rate

The method of “Separation of variables” has used to solve Eq. (1) with periodic variation in time i.e.,

$$V_z(y,t) = \Re e\left\{e^{i\omega t} f_{(y)}\right\} \tag{2}$$

$$\frac{\partial V_z}{\partial t} = \Re e\left\{i\omega e^{i\omega t} f_{(y)}\right\} \tag{3}$$

And

$$\frac{\partial V_z}{\partial y} = \Re e\left\{e^{i\omega t}\left(f'_{(y)}\right)\right\} \tag{4}$$

$$\frac{\partial^2 V_z}{\partial y^2} = \Re e\left\{e^{i\omega t}\left(f''_{(y)}\right)\right\} \tag{5}$$

Putting Eq. (3) and (5) in Eq. (1)

$$\frac{i\omega}{\nu} f_{(y)} = f''_{(y)} \tag{6}$$

With Boundary Conditions

BC1 : at $y = 0$ $\quad f_{(y)} = V$
BC2 : at $y \to \infty$ $\quad f_{(y)} \to 0$

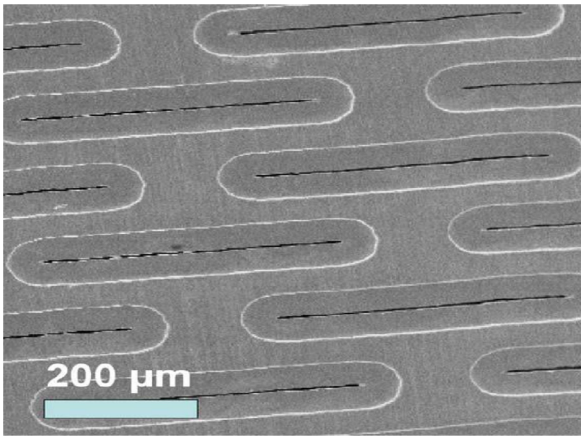

Fig. 2. SEMimage of the slit pore structured membrane.

The general solution of (6) with 2nd Boundary Condition is:

$$f_{(y)} = C\exp\left(-\sqrt{\frac{i\omega}{v}}\, y\right) \tag{7}$$

Applying 1st Boundary Condition:

$$C = V$$

$$f_{(y)} = V\exp\left(-\sqrt{\frac{i\omega}{v}}\, y\right) \tag{8}$$

As

$$V_z(y,t) = \Re e\left\{e^{i\omega t} f_{(y)}\right\}$$

$$V_z(y,t) = \Re e\left\{e^{i\omega t} V\exp\left(-\sqrt{\frac{i\omega}{v}}\, y\right)\right\} \tag{9}$$

Differentiate equation 9 w.r.t. "y",

$$\gamma_{(y)} = \frac{dV_{z(y,t)}}{dy} = \Re e\left\{e^{i\omega t} V\exp\left(-\sqrt{\frac{i\omega}{v}}\, y\right) * \frac{d}{dy}\left(-\sqrt{\frac{i\omega}{v}}\, y\right)\right\} \tag{10}$$

Inserting $\sqrt{\frac{i\omega}{v}} = \lambda$ in Equation (10); the final mathematical equation obtained represented by (11) as:

$$\gamma_{(y)} = \Re e\left\{e^{i\omega t} V\exp(-\lambda\, y).(-\lambda)\right\} \tag{11}$$

Eq. (11) represents the final expression for the present model of submerged membrane. Shear rate on membrane surface can be found by setting boundary condition of "y" i.e., at y=0, represent the shear rate at membrane surface. It can be also observed from Eq. (11), that shear rate is the function of frequency and amplitude of vibration as well as the fluid kinematic viscosity i.e., $\gamma_s = f(\text{amp},\ F, v)$

3. Experimental section

3.1. Oscillating membrane filtration

A food blender that was operated at its highest speed 12 minutes was used to generate oil drops. Size distribution of the oil drops in water was analyesed by Coulter Mullisizier II. The size of the oil drops was found ranging from 1 to 15µm was generated. A 4 µm slit pore structured membrane was used for the filtration of oil from water. The membrane was manufactured from Nickel and its surface was modified with PTFE. The slit pore structure membrane used was provided by Micropore Technologies, UK. A scanning electron microscope (SEM) image of the membrane used is provided in Fig. 2.

Through an oscillating arm the membrane is attached, that is activated by an electrochemical oscillator for the purpose of generating shear rate on surface of the membrane. The schematic diagram of oscillating microfiltration of oil water emulsion separation using oscillating system is presented in Fig. 3. The oscillating system was controlled through a voltage controller purchased from Detla Elektronika with the model no 1464. The frequency that could be generated by oscillating the membrane was in the range of 0–100 Hz while, amplitude could be fixed between0–10 mm. by oscillating membrane in vertical direction the shear rate was created on the outer surface of membrane. The distribution of the shear rate was constant at every point on the membrane surface that was the consequence of the rigid nature of the slit pore membrane. A constant flux of the permeate was obtained using a positive displacement pump.

Filtration tests of crude and vegetable oil drops were evaluated using the oscillating slit pore membrane system at various intensities. Shear rate varied with the oscillation frequency;therefore, filtration experiments were carried out with a vast range of frequency. Further,

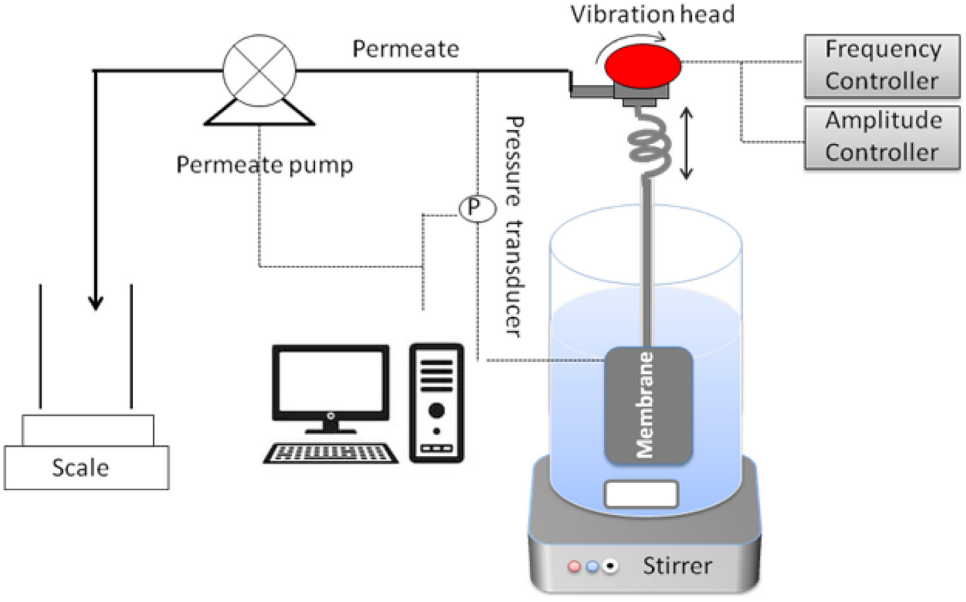

Fig. 3. Schematic diagram of oscillating/vibrating microfiltration unit.

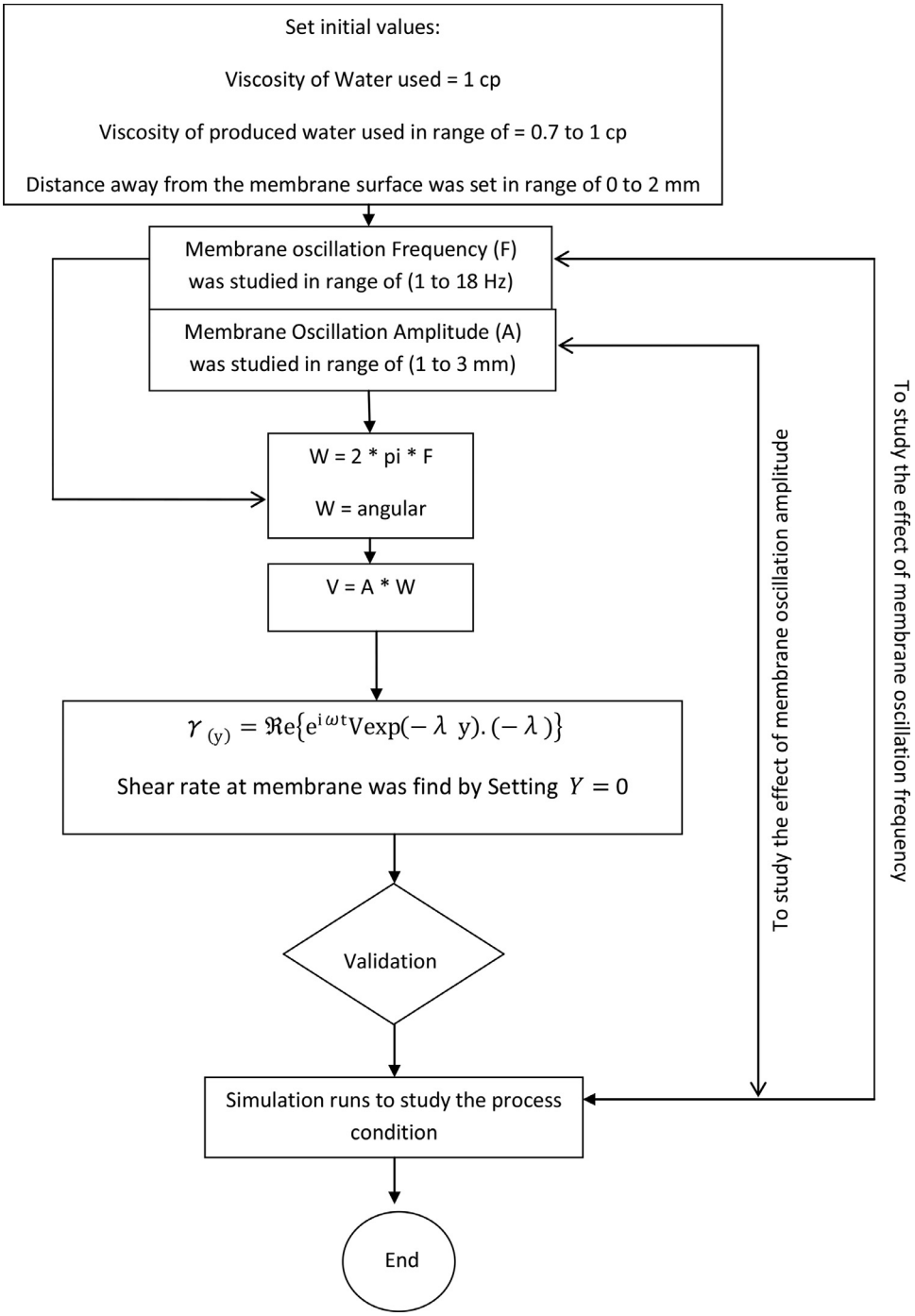

Fig. 4. MATLAB codingfor the shear rate generation as a result of membrane oscillation.

variation in the oscillation amplitude and viscosity was also considered as an important part of the study.

4. Results and discussions

4.1. Computational simulation of the model

All the mathematical/analytical correlations in the form of Eqs. (1) to (11) were integrated into a single model. The analytical model was developed and scripted in MATLAB®. Three parameters: oscillation frequency, amplitude and surrounding fluid viscosity were taken into account in the proposed model. A wide range of frequency values (1 to 18 Hz) were feed into the model, keeping the amplitude constant. Three different values of amplitude (1, 2 and 3 mm) were tested in the model keeping frequency constant. It was found that in the literature that viscosity of produced water ranges from 0.7 to 1 cp at room temperature, therefore, both highest and lowest viscosity values were used in the study. The simulation was run as per the algorithm described in the Fig. 4:

4.2. Oscillation frequency and shear rate

The influence of the oscillation frequency over the shear rate has been investigated keeping the amplitude constant and changing the frequency. In the first set of data (Fig. 5a-c), the amplitude was kept constant and frequency had been changed one increment: 1 Hz, 2 Hz, 3 Hz……6 Hz. The aim was to evaluate the influence of incrementally increasing the frequency on the shear over the membrane surface

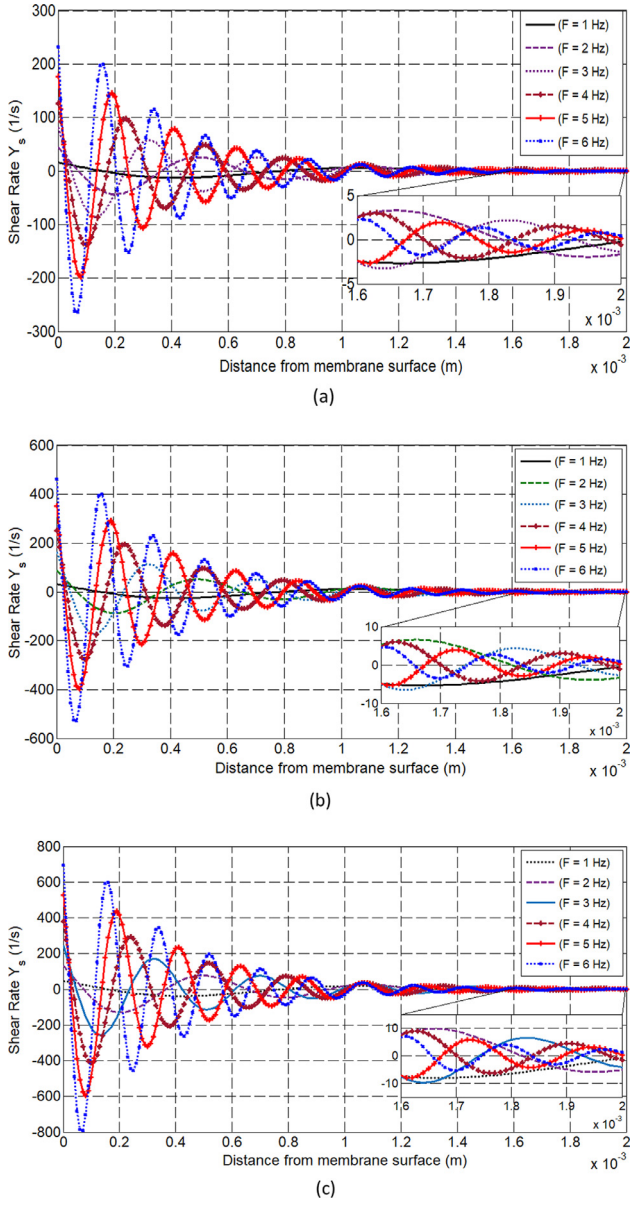

Fig. 5. (a). Shear rate generation on the membrane surface and away from the membrane surface at different membrane oscillation frequencies (1,2,3,4,5 and 6 Hz) and 1 mm Amplitude. (b). Shear rategeneration on the membrane surface and away from the membrane surface at different membrane oscillation frequencies at 2 mm Amplitude. (c). Shear rate generation on the membrane surface and away from the membrane surfaceat different membrane oscillation frequencies and 3 mm Amplitude.

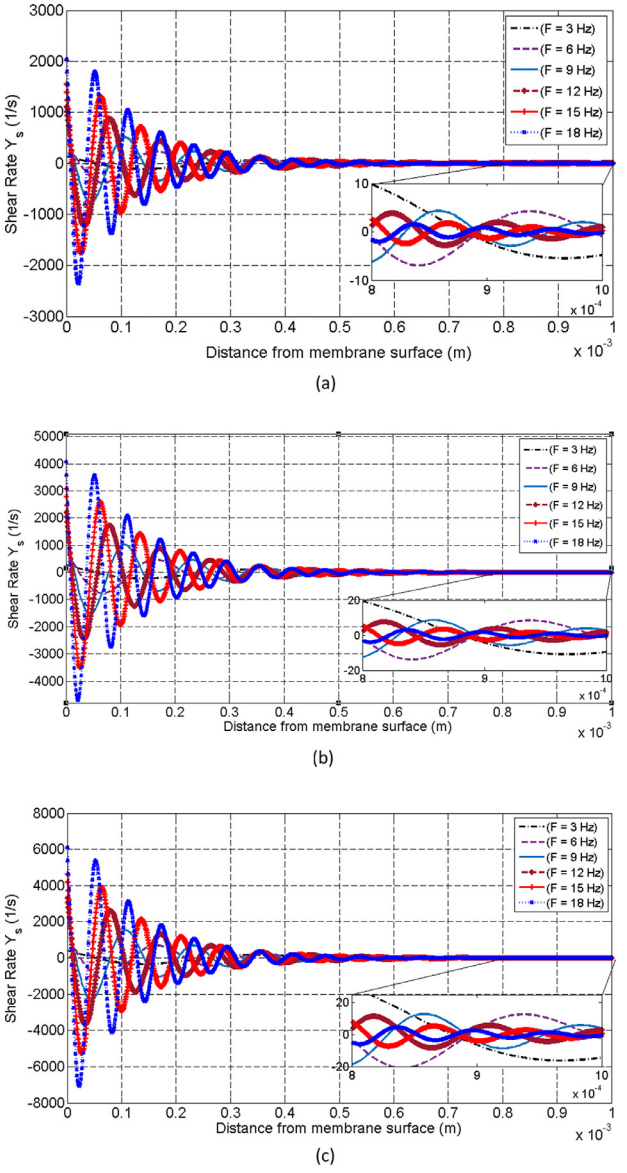

Fig. 6. (a). Shear rate generation on the membrane surface and away from the membrane surface at different membrane oscillation frequencies (from 3 Hz to 18 Hz) and 1 mm Amplitude. (b). Shear rate generation on the membrane surface and away from the membrane surface at different membrane oscillation frequencies (from 3 Hz to 18 Hz) and 2 mm Amplitude. (c). Shear rate generation on the membrane surface and away from the membrane surface at different membrane oscillation frequencies (from 3 Hz to 18 Hz) and Amplitude of 3 mm.

and way from the surface. The oscillation frequency was increase from 1 Hz to 2 Hz and so on to see how change in frequency can alter the shear distribution on the membrane surface and distance away from the membrane surface. Similarly, in the second set of data(Fig. 6(a-c)), the amplitude was kept constant and frequency was changed 3 increments: 3 Hz, 6 Hz, 9 Hz…….18 Hz.

In Fig. 5a amplitude was kept constant at 1 mm, while frequency was changed incrementally one step using water as a surrounding fluid. Zero distance in the figures represents shear rate on the membrane surface. It can be seen in Fig. 5a that at 1 Hz frequency, the generated shear was nearly negligible: about 10 s^{-1} on the membrane surface and diminished to zero at 6mm distance from the membrane surface. Interms of shear, a slightly better result was achieved at 2 Hz frequency where on the membrane surface the shear rate about 30 s^{-1} and diminished to zeroat 1.5 mm distance from the membrane surface. Similarly, at 3 Hz frequency, the shear rate over the membrane surface was about 75 s^{-1} and diminished to zero at around 1.6 mm away from the surface. This shows that one step incrementally enhancement in frequency, shear rate generation over the membrane surface is not consistent. It means that increase in frequency from 1 Hz to 2 Hz gives shear rate different than increasing frequency from 2 Hz to 3 Hz and so on. Althoughat various oscillation frequencies, the shear rate diminished to zero nearly at same point away from the membrane. A similar trend has been observed with oscillation frequencies of 4, 5 and 6 Hz.

Fig. 5(b) and (c) show shear rate against distance from the membrane surface at various frequencies and amplitude of 2 mm and 3 mm respectively. It can be seen in Fig. 5(b) and (c) that a similar trend of shear generation like the previous case (presented in Fig. 5(a) was followed.

The only point when the shear diminished to zero was slightly further away from the origin. Also, it was noticed that increase in the amplitude had a direct relation with the point where the shear diminished to zero.

Keeping the amplitude constant andincreasing the frequencygradually by anincrement of 3: 3,6,9……18 Hz. The aim was to find the behavior of the generated shear rate when membrane was oscillated at higher frequencies. Fig. 6(a-c) show shear rate against distance from the membrane surface at various frequencies and amplitude of 1, 2 and 3 mm respectively. It can be seen in Fig. 6(a-c) that the generation of the shear on the membrane surface is not consistent with the gradual increment of 3. Increase in the shear ratewas like the same as observed in 1 increment enhancement in frequency. At 3 increments increase in frequency the intensity of the shear is high but the shear waves that propagate away from the membrane surface diminished to zero relatively smaller distance (about 0.5 mm) away from the membrane surface as compared to 1 increment increase in frequency. Interestingly, at higher frequencies (15 and 18 Hz), shear on the membrane surface was much higher than generated at lower frequencies but the shear waves diminished to zero nearly the same distance away from the membrane surface. This emphasizes that at higher frequencies, the process could be beneficial in-terms of shear generation over the membrane surface and would lead towards mitigation in the fouling. Also, a lower turbulence would be created in the surrounding fluid.

4.3. Oscillation amplitude and shear rate

In order to investigate the influence of amplitude on shear rate, the oscillation frequency was kept constant and the amplitude was increased incrementally (1, 2 and 3 mm). The 1, 2 and 3 mm amplitude mean distance from the center (up or downward oscillation distance). The process was repeated with various frequencies (1, 3, 6, 9, 12, 15 and 18 Hz)as shown in Fig. 7(a-d). At a frequency of 1 Hz and amplitude of 1, 2 and 3 mm, the generated shear on the membrane surface is 15, 30 and 45 s^{-1} respectively (Fig. 7a). The shear waves propagate away from the membrane surface and its intensity decreased with distance away from the membrane surface. This shows that at a frequency of 1 Hz, the shear distribution is consistent with gradual incrementof 1 in the amplitude. At a distance of 2 mm from the membrane surface, the shear waves still existed. Similarly, at a frequency of 2 and 3 Hz (Fig. 7b, Fig. 7c), the shear generation over the membrane surface is consistent and again the waves propagated away from the membrane surface and existed at a distance of 2 mm. However, at higher frequencies (6, 9….18 Hz), the generated shear over the membrane surface was consistent with the incremental increase in the amplitude but the intensity of the shear decreased drastically as the waves propagates from the surface. See supplementary data for 9 Hz and un-ward frequencies.

4.4. Surrounding fluid viscosity and shear rate

The influence of fluid viscosity is important on the shear generation and investigated by various researchers (Sun et al., 2020; Zhu, Wang, et al., 2021; Zhu, Zhong, et al., 2021). Various values of surrounding fluid viscosities were tested in the model inorder to evaluate the influence of viscosity on the shear rate. Room temperature viscosity values for water and produced water were used. Viscosity of produced water ranges from 0.7 to 1 cp(Fakhru'l-Razi et al., 2009), therefore, minimum and maximum values were tested. Fig. 8a and Fig. 8b show shear rate against distance from the membrane surface at 1 cp and 0.7 cprespectivelyat various oscillation frequencies and amplitude of 2 mm. It has been observed that higher shear rate on the membrane surface was created in the lower viscosity (0.7 cp) in comparison with the higher viscosity system (1cp). Shear rate of around 630 s^{-1} was noticed in 1 cp fluid viscosity system at the membrane surface under oscillation frequency of 6 Hz and amplitude of 2 mm. On the other hand, using the same conditions (6 Hz Frequency and 2 mm amplitude) the generated shear on the membrane surface was around 800 s^{-1} when 0.7 cp fluid viscosity was

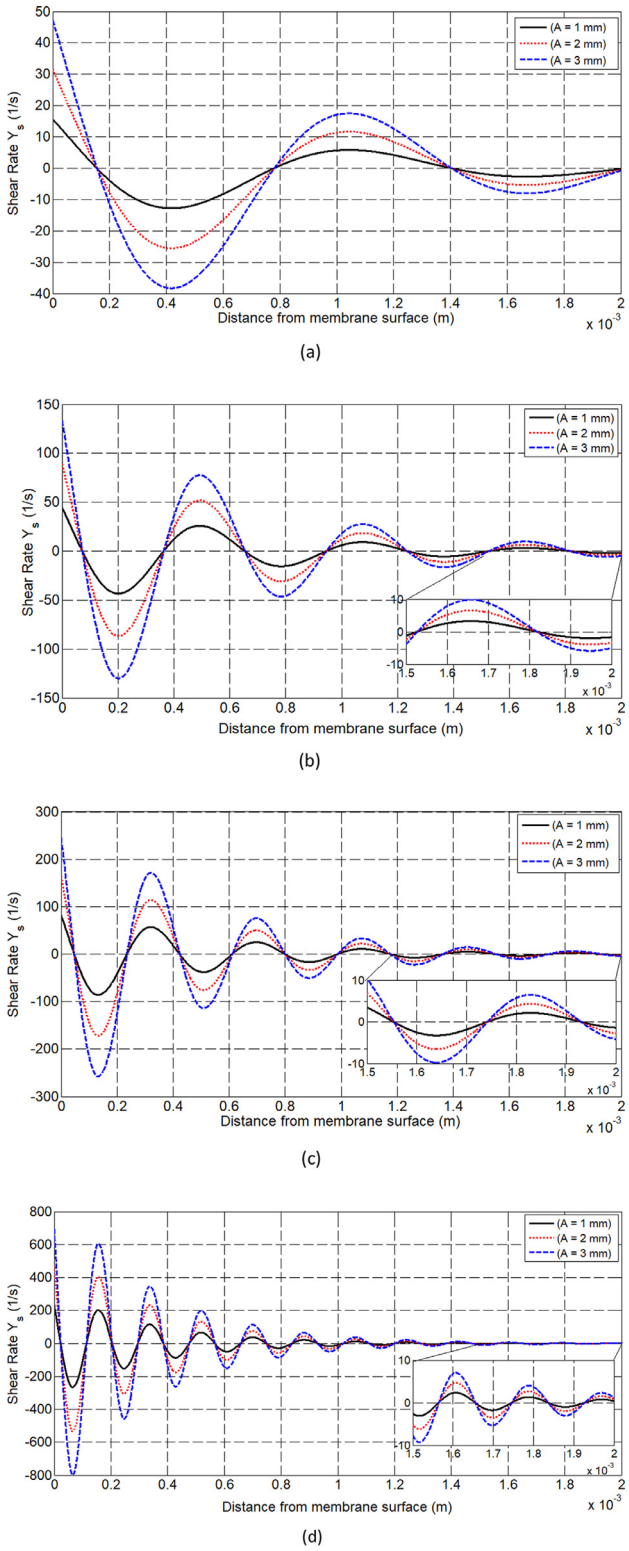

Fig. 7. (a). Shear rategeneration on the membrane surface and away from the membrane surface at different membrane oscillation amplitude and frequency of 1 Hz. (b). Shear rate generation on the membrane surface and away from the membrane surfaceat different membrane oscillation amplitude and frequency of 2 Hz. (c). Shear rate generation on the membrane surface and away from the membrane surfaceat different membrane oscillation amplitude at frequency of 3 Hz. (d). Shear rate generation on the membrane surface and away from the membrane surfaceat different membrane oscillation amplitude and frequency of 6 Hz.

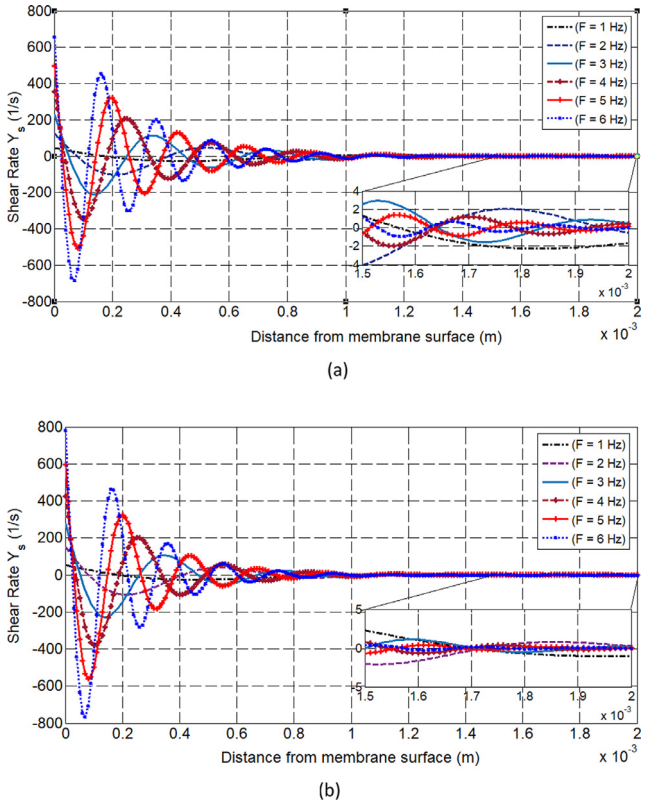

Fig. 8. (a). Shear rate generation on the membrane surface and away from the membrane surface at different membrane oscillation frequencies and 2 mm Amplitude using surrounding fluid viscosity 1 cp. (b). Shear rate generation on the membrane surface and away from the membrane surface at different membrane oscillation frequencies and 2 mm Amplitude using surrounding fluid viscosity of 0.7 cp.

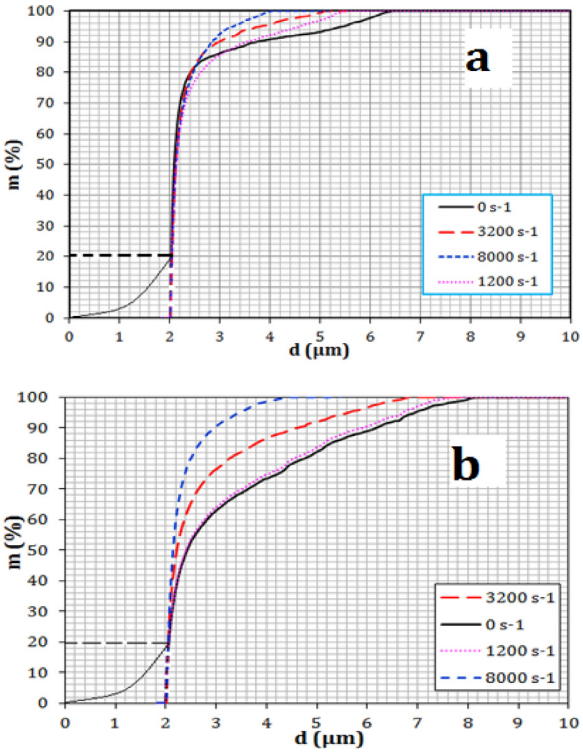

Fig. 9. Size distribution by mass of Tween 20 stabilized oil drops in the permeate (a) at 200 lm^{2}hr^{-1} and (b) 1000 lm^2 hr$^{-1.}$

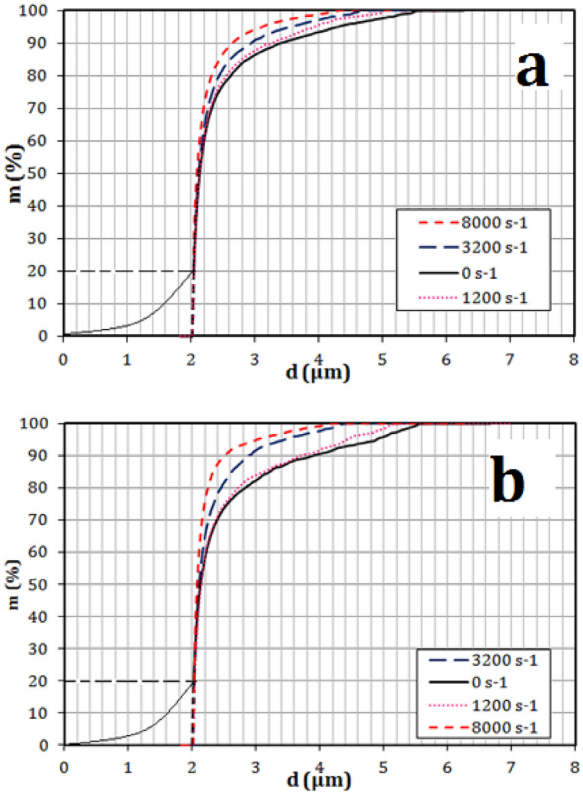

Fig. 10. Size distribution by mass of crude oil drops in the permeate (a) at 200 lm^2 hr^{-1} and (b) 1000 lm^2 hr^{-1}.

used. Further, the shear waves propagated at a higher intensity away from the membrane surface when lowerfluid viscosity system (0.7 cp) was used as compared to higher viscosity system (1 cp). Also, the shear waves diminished to zero further away from the membrane surface at lower fluid viscosity system. Lower shear on the membrane surface at higher viscosity may be due to the greater cohesion among the molecule in the surrounding fluid (Dezhi et al., 1999; Eow et al., 2001). The layers in the fluid with higher viscosity are tightly bonded and therefore, this leads the to a higher resistance to the propagation of shear waves away from the surface and diminished to zero quickly (Dezhi et al., 1999; Eow et al., 2001).

4.5. Model validation with experimental results

Shear rate over the membrane surface because of the oscillation generate a lift that leads particles or drops away from the membrane surface (Ullah, Holdich, et al., 2012a). As a consequence, the deposition of particles on the membrane surface is minimized and therefore fouling is mitigated (Postlethwaite et al., 2004). The model has been validated with the experimental results showing a smaller concentration of oil drops in the permeate as a consequence of the shear rate application over the membrane surface has been observed. Oil drops stabilised by Tween 20 and crude oil drops were used. Oil drops stabilised by Tween and crude oil drops provided interfacial tension of 4 and 30 mnm^{-1} respectively. Size distributions based on mass of oil drops in the permeate are provided in Fig. 9 and Fig. 10. It is clear from Fig. 9 and Fig. 10 that a significent decrease in the permeate concentration occured incase of membrane oscillation. Decrease in the concentration was found to be a linear function of the applied shear. Also, interfacial tension played a

Table 1
No of drops in the permeate and permeate concentration (ppm) observed at crude oil drops at 200 lm^2hr^{-1}.

Shear rate (s^{-1})	No of drops per 0.4 ml sample	Concentration of crude oil in the feed (ppm)	Concentration of crude oil in the permeate (ppm)
10,000	1020	400	5
8000	1606	400	7
0	5092	400	21

vital role in oil concentration in the permeate. At lower interfacial tension, squeezing and distoration of the drops was easy and therefore, the drops pass easily into the permeate (Ullah et al., 2019; Ullah, Holdich, et al., 2012b). On the other hand, at higher interfacial tension the drops were more rigid in nature and its distoration and squeezing was difficult and that's way a lower portion of the oil drops passed into the permeate (Jiménez et al., 2018). Further, increase in the permeate flux enhanced resistance towards the lift away from membrane surface generated by shear, therefore, a higher concentration in the permeate was noticed when the permeate flux was increased. Also, number of drops in the permeate decreased when shear was applied to the memrbane surface.

The permeate size distribution is supported by theno of oil drops concentration of oil content (ppm) in the permeate provided in Table 1. A significant reduction in number of oil drops in the permeate were observed in increase in shear rate. Oil drops reduced from around 6000 to 1000 at 0 and 10,000 s^{-1} shear rate. Further, oil concentration in the permeate was measurable reduced with increase in shear rate. Four times greater concentration in the permeate was noticed without applied shear rate as compared to 10,000 s^{-1} shear rate.

Slot/pore blocking of the membrane was also assessed experimentally with the application of the shear rate to the membrane surface. For the pore blocking experiments again vegetable oil drops stabilized with the Tween 20 and crude oil drops were used. It was found that like permeate concentration pore blocking has also been influenced by the application of the shear rate as a consequence of the membrane oscillation. Pore blocking considerably decreased with the application of the shear rate (Fig. 11). Decrease in the pore blocking was evaluated as a linear function of the oscillation frequency: higher the oscillation frequency lower pore blocking was observed. Similarly, the interfacial tension was also important in the pore blocking. Under the same condition, the oil drops with lower interfacial tension the oil drops deformed and passed through the membrane and contributed less to the pore blocking (Ullah et al., 2019). On the other hand, pore blocking was higher at higher interfacial tension, the drops were more rigid in nature, were more difficult to squeeze through the pore and contributed more towards pore blocking (Ullah et al., 2019; Ullah, Holdich, et al., 2012b).

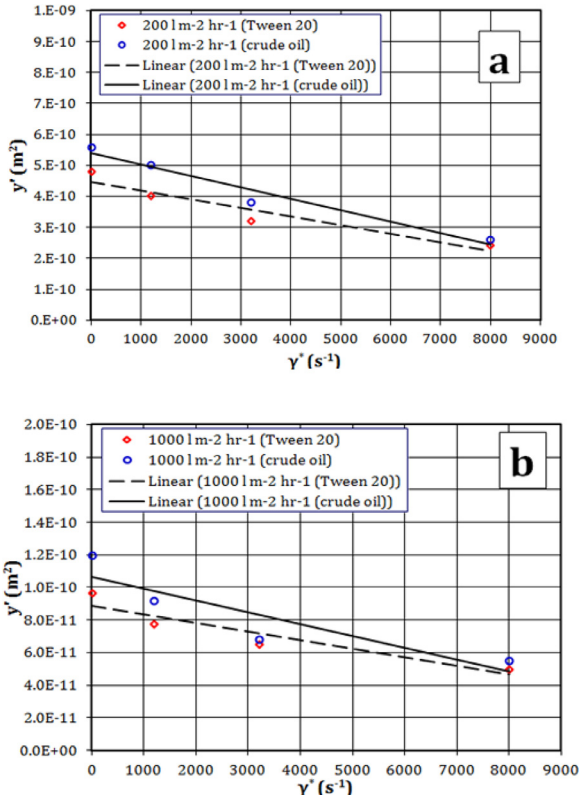

Fig. 11. The influence of shear rate on the pore blocking using Tween 20 stabilized vegetable oil drops and crude oil drops at(a) 200 l m^{-2} h^{-1} and (b) 1000 l m^{-2} h^{-1}.

5. Conclusions

A novel analytical approach has been developedbased on Stokes boundary layer equation. The model took membrane oscillation frequency, amplitude and surrounding fluid viscosity into account. It was found that incremental increase in membrane oscillation frequency and amplitude behaved differently interms of shear generation over the surface and away from the surface. Enhancement in the shear rate as a consequence of the incremental increase (1 Hz increase) in oscillation frequency was not consistent on the membrane surface. It means that increase in oscillation frequency from 1 Hz to 2 Hz generated different shear rate as compare to increase in frequency from 2 Hz to 3 Hz. Although, the shear waves diminished to zero nearly the same distance away from the membrane as a result of increase in the frequency incrementally. A consistent enhancement in the shear rate on the membrane surface was noticed as result of incrementally increase in the amplitude (1 mm increase, for example 1 mm, 2 mm and so on). By increasing frequency from 1 Hz to 2 Hz, shear rate changed from 10 s^{-1} to 30 s^{-1}. While, changing frequency from 2 Hz to 3 Hz, shear rate jumped from 30 to 75 s^{-1}. The difference in shear rate was 20 s^{-1} in case of increase in frequency from 1 Hz to 2 Hz and 35 s^{-1} shear rate increase was noticed by enhancing frequency from 2 to 3 Hz. However, the shear waves diminished to zero at a larger distance as compared in case of incremental increase in the amplitude as compared to 1 step enhancement in frequency. Membrane oscillation frequency was found to be effective in terms of shear generation on the membrane surface rather than amplitude. Not only on the surface greater shear was generated but also a lower turbulence was created in the surrounding fluidbecause of enhancement in oscillation frequency as compared to the amplitude. Further, with lower fluid viscosity (0.7 cp) the intensity of shear over the membrane surface was greater that allowed the waves to propagate at a larger distance as compared to higher viscosity systems (1 cp). The analytical study conducted was validated with the experimental results and it was found that membrane oscillation decreased oil drop concentration in the permeate. Decrease in oil concentration in the permeate was found to be a linear function of the oscillation frequency. Moreover, a lower number of drops in the permeate was noted because of the mem-

brane oscillation. Furthermore, shear rate influenced the pore blocking, higher the intensity of the shear, lower the pore blocking was noticed.

Declaration of Competing Interest

The authors declare that they have no known competing financial interests or personal relationships that could have appeared to influence the work reported in this paper.

Acknowledgments

The authors would like to thank University of Engineering and Technology Peshawar, Pakistan and Higher Education Commission Pakistan for financially supporting the study.

References

Beier, S.P., Jonsson, G., 2007. Separation of enzymes and yeast cells with a vibrating hollow fiber membrane module. Sep. Purif. Technol. 53, 111–118.
Bellhouse, B.J., Sobey, I.J., Alani, S., DeBlois, B.M., 1994. Enhanced filtration using flat membranes and standing vortex waves. Bioseparation 4, 127–138.
Bilstad, T., Espedal, E., 1996. Membrane separation of produced water. Water Sci. Technol. 34, 239–246.
Chakrabarty, B., Ghoshal, A.K., Purkait, M.K., 2008. Ultrafiltration of stable oil-in-water emulsion by polysulfone membrane. J. Memb. Sci. 325, 427–437.
Chandler, M., Zydney, A., 2006. Effects of membrane pore geometry on fouling behavior during yeast cell microfiltration. J. Memb. Sci. 285, 334–342.
Cheryan, M., Rajagopalan, N., 1998. Membrane processing of oily streams. Wastewater treatment and waste reduction. J. Memb. Sci. 151, 13–28.
Cui, Z.F., Chang, S., Fane, A.G., 2003. The use of gas bubbling to enhance membrane processes. J. Memb. Sci. 221, 1–35.
Cumming, I.W., Holdich, R.G., Smith, I.D., 2000. The rejection of oil by microfiltration of a stabilised kerosene/water emulsion. J. Memb. Sci. 169, 147–155.
Dezhi, S., Chung, J.S., Xiaodong, D., Ding, Z., 1999. Demulsification of water-in-oil emulsion by wetting coalescence materials in stirred-and packed-columns. Colloids Surfaces A Physicochem. Eng. Asp. 150, 69–75.
Eow, J.S., Ghadiri, M., Sharif, A.O., Williams, T.J., 2001. Electrostatic enhancement of coalescence of water droplets in oil: a review of the current understanding. Chem. Eng. J. 84, 173–192.
Fakhru'l-Razi, A., Pendashteh, A., Abdullah, L.C., Biak, D.R.A., Madaeni, S.S., Abidin, Z.Z., 2009. Review of technologies for oil and gas produced water treatment. J. Hazard. Mater. 170, 530–551.
Faksness, L.-G., Grini, P.G., Daling, P.S., 2004. Partitioning of semi-soluble organic compounds between the water phase and oil droplets in produced water. Mar. Pollut. Bull. 48, 731–742.
Falahati, H., Tremblay, A.Y., 2011. Flux dependent oil permeation in the ultrafiltration of highly concentrated and unstable oil-in-water emulsions. J. Memb. Sci. 371, 239–247.
Genkin, G., Waite, T.D., Fane, A.G., Chang, S., 2006. The effect of vibration and coagulant addition on the filtration performance of submerged hollow fibre membranes. J. Memb. Sci. 281, 726–734.
Gomaa, H., Al Taweel, A.M., 2004. Dynamic analysis of mass transfer at vertically oscillating surfaces. Chem. Eng. J. 102, 71–82.
Gomaa, H., Al Taweel, A.M., 2005. Effect of oscillatory motion on heat transfer at vertical flat surfaces. Int. J. Heat Mass Transf. 48, 1494–1504.
Gomaa, H., Al Taweel, A.M., Landau, J., 2004. Mass transfer enhancement at vibrating electrodes. Chem. Eng. J. 97, 141–149.
Gomaa, H.G., Taweel, A.M.Al., 2007. Intensification of inter-phase mass transfer: the combined effect of oscillatory motion and turbulence promoters. Heat mass Transf 43, 371.
Herman, C., Kang, E., 2001a. Comparative evaluation of three heat transfer enhancement strategies in a grooved channel. Heat mass Transf 37, 563–575.
Herman, C., Kang, E., 2001b. Experimental visualization of temperature fields and study of heat transfer enhancement in oscillatory flow in a grooved channel. Heat mass Transf 37, 87–99.
Holdich, R.G., Cumming, I.W., Smith, I.D., 1998. Crossflow microfiltration of oil in water dispersions using surface filtration with imposed fluid rotation. J. Memb. Sci. 143, 263–274.
Huang, S., Ras, R.H.A., Tian, X., 2018. Antifouling membranes for oily wastewater treatment: Interplay between wetting and membrane fouling. Curr. Opin. Colloid Interface Sci. 36, 90–109.
Jepsen, K.L., Bram, M.V., Pedersen, S., Yang, Z., 2018. Membrane fouling for produced water treatment: a review study from a process control perspective. Water 10, 847.
Jiménez, S., Micó, M.M., Arnaldos, M., Medina, F., Contreras, S., 2018. State of the art of produced water treatment. Chemosphere 192, 186–208.
Kuiper, S, Brink, R., Nijdam, W., Krijnen, G.J.M., Elwenspoek, M.C., 2002. Ceramic microsieves: influence of perforation shape and distribution on flow resistance and membrane strength. J. Memb. Sci. 196, 149–157.
Kuiper, Stein, van Rijn, C., Nijdam, W., Raspe, O., van Wolferen, H., Krijnen, G., Elwenspoek, M., 2002. Filtration of lager beer with microsieves: flux, permeate haze and in-line microscope observations. J. Memb. Sci. 196, 159–170.
Lee, S., Aurelle, Y., Roques, H., 1984. Concentration polarization, membrane fouling and cleaning in ultrafiltration of soluble oil. J. Memb. Sci. 19, 23–38.
Lipp, P., Lee, C.H., Fane, A.G., Fell, C.J.D., 1988. A fundamental study of the ultrafiltration of oil-water emulsions. J. Memb. Sci. 36, 161–177.
Lu, D., Zhang, T., Ma, J., 2015. Ceramic membrane fouling during ultrafiltration of oil/water emulsions: roles played by stabilization surfactants of oil droplets. Environ. Sci. Technol. 49, 4235–4244.
Mackley, M.R., Stonestreet, P., 1995. Heat transfer and associated energy dissipation for oscillatory flow in baffled tubes. Chem. Eng. Sci. 50, 2211–2224.
Mohammadi, T., Kazemimoghadam, M., Saadabadi, M., 2003. Modeling of membrane fouling and flux decline in reverse osmosis during separation of oil in water emulsions. Desalination 157, 369–375.
Nabi, N., Aimar, P., Meireles, M., 2000. Ultrafiltration of an olive oil emulsion stabilized by an anionic surfactant. J. Memb. Sci. 166, 177–188.
Nazzal, F.F., Wiesner, M.R., 1996. Microfiltration of oil-in-water emulsions. Water Environ. Res. 68, 1187–1191.
Ni, X., Mackley, M.R., Harvey, A.P., Stonestreet, P., Baird, M.H.I., Rao, N.V.R., 2003. Mixing through oscillations and pulsations—a guide to achieving process enhancements in the chemical and process industries. Chem. Eng. Res. Des. 81, 373–383.
Padaki, M., Murali, R.S., Abdullah, M.S., Misdan, N., Moslehyani, A., Kassim, M.A., Hilal, N., Ismail, A.F., 2015. Membrane technology enhancement in oil–water separation. A review. Desalination 357, 197–207.
Partovinia, A., Naeimpoor, F., 2013. Phenanthrene biodegradation by immobilized microbial consortium in polyvinyl alcohol cryogel beads. Int. Biodeterior. Biodegradation. 85, 337–344.
Partovinia, A., Naeimpoor, F., 2014. Comparison of phenanthrene biodegradation by free and immobilized cell systems: formation of hydroxylated compounds. Environ. Sci. Pollut. Res. 21, 5889–5898.
Patterson, J. W., 1985. *Industrial wastewater treatment technology*.
Peng, H., Volchek, K., MacKinnon, M., Wong, W.P., Brown, C.E., 2004. Application on to nanofiltration to water management options for oil sands operation. Desalination 170, 137–150.
Pope, J.M., Yao, S., Fane, A.G., 1996. Quantitative measurements of the concentration polarisation layer thickness in membrane filtration of oil-water emulsions using NMR micro-imaging. J. Memb. Sci. 118, 247–257.
Postlethwaite, J., Lamping, S.R., Leach, G.C., Hurwitz, M.F., Lye, G.J., 2004. Flux and transmission characteristics of a vibrating microfiltration system operated at high biomass loading. J. Memb. Sci. 228, 89–101.
Rezakazemi, M., Khajeh, A., Mesbah, M., 2018. Membrane filtration of wastewater from gas and oil production. Environ. Chem. Lett. 16, 367–388.
Salon, S., Armenio, V., Crise, A., 2007. A numerical investigation of the Stokes boundary layer in the turbulent regime. J. Fluid Mech. 570, 253.
Sarrade, S., Schrive, L., Gourgouillon, D., Rios, G.M., 2001. Enhanced filtration of organic viscous liquids by supercritical CO_2 addition and fluidification. Application to used oil regeneration. Sep. Purif. Technol. 25, 315–321.
Sun, N., Zhu, Z., Zeng, G., 2020. Bioinspired superwetting fibrous skin with hierarchical roughness for efficient oily water separation. Sci. Total Environ. 744, 140822.
Ullah, A., Ahmad, J., Khan, H., Khan, S.W., Zamani, F., Hasan, S.W., Starov, V.M., Chew, J.W., 2019. Membrane oscillation and slot (pore) blocking in oil–water separation. Chem. Eng. Res. Des. 142, 111–120.
Ullah, A., Habib, M., Khan, S.W., Ahmad, M.I., Starov, V.M., 2015. Membrane oscillation and oil drop rejection during produced water purification. Sep. Purif. Technol. 144, 16–22.
Ullah, A., Holdich, R.G., Naeem, M., Khan, S.W., Starov, V.M., 2014. Prediction of size distribution of crude oil drops in the permeate using a slotted pore membrane. Chem. Eng. Res. Des. 92, 2775–2781.
Ullah, A., Holdich, R.G., Naeem, M., Starov, V.M., 2012a. Shear enhanced microfiltration and rejection of crude oil drops through a slotted pore membrane including migration velocities. J. Memb. Sci. 421, 69–74.
Ullah, A., Holdich, R.G., Naeem, M., Starov, V.M., 2012b. Stability and deformation of oil droplets during microfiltration on a slotted pore membrane. J. Memb. Sci. 401, 118–124.
Ullah, A., Khan, S.W., Shakoor, A., Starov, V.M., 2013. Passage and deformation of oil drops through non-converging and converging micro-sized slotted pore membranes. Sep. Purif. Technol. 119, 7–13.
Ullah, A., Shahzada, K., Khan, S.W., Starov, V., 2020. Purification of produced water using oscillatory membrane filtration. Desalination 491, 114428.
Ullah, A., Starov, V.M., Naeem, M., Holdich, R.G., 2011. Microfiltration of deforming oil droplets on a slotted pore membrane and sustainable flux rates. J. Memb. Sci. 382, 271–277.
Ullah, A., Starov, V.M., Naeem, M., Holdich, R.G., Semenov, S., 2013. Filtration of suspensions using slit pore membranes. Sep. Purif. Technol. 103, 180–186.
van Rijn, C. J. M., Veldhuis, G. J., & Kuiper, S., 1998. Nanosieves with microsystem technology for
Widodo, S., Ariono, D., Khoiruddin, K., Hakim, A.N., Wenten, I.G., 2018. Recent advances in waste lube oils processing technologies. Environ. Prog. Sustain. Energy. 37, 1867–1881.
Zhu, Y., Wang, D., Jiang, L., Jin, J., 2014. Recent progress in developing advanced membranes for emulsified oil/water separation. NPG Asia Mater 6 e101–e101.
Zhu, Z., Wang, W., Zhang, Q., Chen, X., 2021. Insight into the feed/permeate flow velocity on the trade-off of water flux and scaling resistance of superhydrophobic and welding-pore fibrous membrane in membrane distillation. J. Memb. Sci. 620, 118883.
Zhu, Z., Zhong, L., Horseman, T., Liu, Z., Zeng, G., Li, Z., Lin, S., Wang, W., 2021. Superhydrophobic-omniphobic membrane with anti-deformable pores for membrane distillation with excellent wetting resistance. J. Memb. Sci. 620, 118768.